

Performances of BATS and CLM land-surface schemes in RegCM4 in simulating precipitation over CORDEX Southeast Asia domain

Jing Xiang Chung,^a  Liew Juneng,^a Fredolin Tangang^{a,b*}  and Ahmad F. Jamaluddin^{a,c}

^a School of Environmental and Natural Resource Sciences, Faculty of Science and Technology, Universiti Kebangsaan Malaysia, Bangi, Malaysia

^b Center of Regional Climate Change and Renewable Energy (RU-CORE), Ramkhamhaeng University, Bangkok, Thailand

^c Malaysian Meteorological Department, Petaling Jaya, Malaysia

ABSTRACT: This study evaluates the sensitivity of precipitation in Southeast Asia (SEA) to the choice of land-surface schemes available in RegCM4, that is BATS1e (BATS) and CLM4.5 (CLM), over the CORDEX SEA domain. Two similar simulations using different land-surface schemes were conducted for the period 1989 to 2007, with a horizontal resolution of 25×25 km. Four different types of observational data were used to evaluate the performance of these simulations. It was found that both of these simulations reproduced the SEA precipitation climatology spatial patterns reasonably well. However, the BATS simulation systematically produced higher frequency and more intense precipitation over land. The CLM simulation, although overestimating the precipitation frequency, produced a lower amount of on-land precipitation. The precipitation annual cycle and interannual variability were both insensitive to the choice of land-surface scheme. The errors in the precipitation simulation were found to originate from the simulated convective precipitation (CPr). Large-scale precipitation was found to be less sensitive to the choice of land-surface scheme. The influence of the land-surface scheme on SEA precipitation simulation took place through the interaction between soil moisture content and CPr. The soil moisture content was consistently higher in the BATS simulation, as was the CPr simulated. During December to February (DJF), the difference in the precipitation amount simulated by BATS and CLM simulations was lower over the SEA mainland, even though the soil moisture content in both simulations was very different. This difference was due to the inactivity of the convective activities over the SEA mainland during DJF. This study concludes that the simulation of SEA precipitation amount was sensitive to the choice of land-surface scheme, and recommend the use of CLM4.5 land-surface scheme for simulation of SEA precipitation.

KEY WORDS CORDEX Southeast Asia; Southeast Asia precipitation; land-surface scheme; RegCM

Received 4 August 2016; Revised 25 May 2017; Accepted 19 June 2017

1. Introduction

Precipitation is one of the most difficult parameters to simulate as it is a highly complex process which involves the interaction between atmospheric motion, thermodynamics, clouds microphysics and other hydrometeors (Emori *et al.*, 2001). However, the accuracy of the precipitation simulation is important in reproducing a realistic climate in models (e.g. Giorgi *et al.*, 1993; Osborn and Hulme, 1997) as its bias can influence the water balance (Li *et al.*, 2016) and the general circulation in the model (e.g. Arakawa, 2004; Fekete *et al.*, 2004). Thus, optimizing the regional climate model (RCM) to allow realistic simulation precipitation is important, especially when the model is to be used to downscale future climate change information from general circulation models (GCM). For this purpose, numerous studies have been conducted to

optimize the RCM either by determining the best combination of existing physics schemes to be used for a certain region (e.g. Kalognomou *et al.*, 2013; Kang *et al.*, 2014; Reboita *et al.*, 2014; Gao *et al.*, 2016; Juneng *et al.*, 2016; Li *et al.*, 2016; Ngo-Duc *et al.*, 2017), or by introducing new or modifying current physics parameterization schemes (e.g. Chow *et al.*, 2006; Zou *et al.*, 2014; Gianotti and Eltahir, 2014a, 2014b).

Southeast Asia (SEA) is a region which is exposed to various climate-related hazards, yet efforts towards studying and optimizing the RCM are relatively new and fractured; these studies focus on limited areas within SEA (e.g. Francisco *et al.*, 2006; Salimun *et al.*, 2010; Gianotti *et al.*, 2012; Kwan *et al.*, 2014; Wei *et al.*, 2014; Cruz *et al.*, 2016). Juneng *et al.* (2016) and Ngo-Duc *et al.* (2017) of the Southeast Asia Regional Climate Downscaling (SEACLID)/Coordinated Regional Climate Downscaling Experiment (CORDEX, Giorgi *et al.*, 2009) SEA project have conducted a region-wide model sensitivity test over SEA. In the sensitivity test conducted by Juneng *et al.* (2016), they used six different cumulus

* Correspondence to: F. Tangang, School of Environmental and Natural Resource Sciences, Faculty of Science and Technology, Universiti Kebangsaan Malaysia, Bangi 43600, Selangor, Malaysia.
E-mail: tangang@ukm.edu.my; ftangang@gmail.com

parameterization schemes (CPS) and three different ocean surface schemes in the Regional Climate Model version 4 (RegCM4), developed by the Earth System Physics section of Abdus Salam International Centre for Theoretical Physics (ICTP, Giorgi *et al.*, 2012). They aimed to identify the most suitable combination of CPS and ocean surface schemes for use in simulating SEA precipitation. Of the six CPS used, they observed that CPS MIT-Emanuel (Emanuel and Živković-Rothman, 1999) was the most suitable CPS for SEA precipitation simulation; although this tended to strongly overestimate the amount of precipitation. They also noted that the choice of ocean surface scheme did not have a significant impact on the on-land precipitation simulated.

The identification and selection of the most appropriate CPS to be used in a RCM for climate simulation is a common approach adopted by climate scientists. This is because the conversion of atmospheric moisture to convective precipitation (CPr) at scales unresolvable by the model is governed by the CPS (Li *et al.*, 2016). Thus, the choice of CPS plays an important role in the simulated precipitation. However, for a realistic precipitation simulation, the choice of an appropriate surface latent heat flux-related parameterization scheme is no less important. A surface latent heat flux-related parameterization such as land-surface scheme plays an important role in determining the amount of moisture that goes into the atmosphere from the surface (Li *et al.*, 2016). For the East Asia region, Kang *et al.* (2014) and Li *et al.* (2016) showed that the RegCM4 with CPS MIT-Emanuel responded differently to the simulation of boreal summer precipitation when the model was coupled with the Biosphere–Atmosphere Transfer Scheme (BATS, Dickinson *et al.*, 1993) version 1e and the Community Land Model (CLM) version 3 (Oleson *et al.*, 2004; Steiner *et al.*, 2009). They noticed that the BATS simulation tended to produce a higher amount of boreal summer precipitation compared with the CLM simulation. Similarly, the smaller precipitation bias result for CLM was also achieved over the West African region (Steiner *et al.*, 2009), Central America (Diro *et al.*, 2012), the western Himalayas (Tiwari *et al.*, 2015), the Tibetan Plateau (Wang *et al.*, 2015) and China (Gao *et al.*, 2016). For the tropical region, Reboita *et al.* (2014) noticed that the MIT-Emanuel CPS and CLM combination produced the best precipitation simulation over the Amazon region in South America.

Previous studies conducted over different regions have thus far agreed unanimously on the fact that simulations using CLM as land-surface scheme tend to produce precipitation with smaller bias compared with BATS. Therefore, the strong overestimation of SEA precipitation found by Juneng *et al.* (2016) using MIT-Emanuel simulation was likely due to the BATS land-surface scheme used in their simulation. Thus, the main objective of this study is to compare the performance of RegCM4 in simulating SEA precipitation when the model is coupled to the land-surface scheme using both BATS version 1e and the newer version of CLM (version 4.5) during the boreal winter monsoon (December to February, DJF) and the boreal summer

monsoon (June to August, JJA). This study also investigates the effect that the choice of land-surface scheme has on the simulation of precipitation annual cycle and year-to-year variation over the SEA region.

2. Model and experiment setup

The RegCM4 used in this study was version 4.4.5. Two land-surface schemes, BATS version 1e and CLM version 4.5 (Oleson *et al.*, 2013) were considered in this study while all other physical settings were kept identical. The CPS used for both simulations was the MIT-Emanuel scheme, the non-local planetary boundary layer scheme was that of Holtslag (Holtslag *et al.*, 1990) and the moisture scheme was that of the Subgrid Explicit Moisture (SUBEX) by Pal *et al.* (2007) based on the work of Sundqvist *et al.* (1989). As for the ocean flux scheme, Juneng *et al.* (2016) have shown that the choice of ocean flux scheme does not have a great deal of impact on the simulation of SEA on-land precipitation. However, Li *et al.* (2016) suggest that the Zeng scheme (Zeng *et al.*, 1998) in which the ocean surface roughness length is determined depending on the friction velocity and the effect of viscosity (denoted as Zeng2) is the best for use in the region of East to SEA. Therefore, the Zeng2 scheme was used in both simulations. In addition, for both simulations, the diurnal cycle sea surface temperature scheme was used. All the parameterized values of the physics schemes used were kept at their default values.

The simulation domain in this study spanned from longitude 91.97° to 143.79°E and latitude 12.39°S to 24.51°N, with grid spacing of 25 × 25 km (Figure 1) and 18 sigma levels vertically. This area is the SEACLID/CORDEX SEA official domain. The simulation was forced using the ERA-Interim reanalysis dataset (Dee *et al.*, 2011) with a grid spacing of 1.5° × 1.5° at 6 h intervals for the period 1 January 1989 to 31 December 2007. The results from the first 12 months of the simulations were discarded as the model spin up. Also, data within the buffer region of the domain (Figure 1) were excluded from the analysis.

To validate the performance of the simulations in simulating the precipitation in SEA, four observational datasets were considered in this study. The four datasets used were: (1) Asian Precipitation Highly Resolved Observational Data Integration Towards the Evaluation (APHRODITE) of water resources project (Yatagai *et al.*, 2009) MA V1101 with resolution 0.25° × 0.25°, (2) Climatic Research Unit of the University of East Anglia (CRU, Mitchell and Jones, 2005) TS3.21 with resolution 0.5° × 0.5°, (3) Global Precipitation Climatology Centre precipitation reanalysis dataset (GPCC, Schneider *et al.*, 2014) version 6 with resolution 0.5° × 0.5° and (4) Tropical Rainfall Measuring Mission (TRMM, Huffman *et al.*, 2007) 3B42 version 7 with resolution 0.25° × 0.25°. We refrained from using a particular dataset as a standard dataset for validation since Juneng *et al.* (2016) indicated large variations between various dataset products, especially over the southern region of SEA. TRMM 3A25 version 7 with resolution 0.5° × 0.5° was also used in this

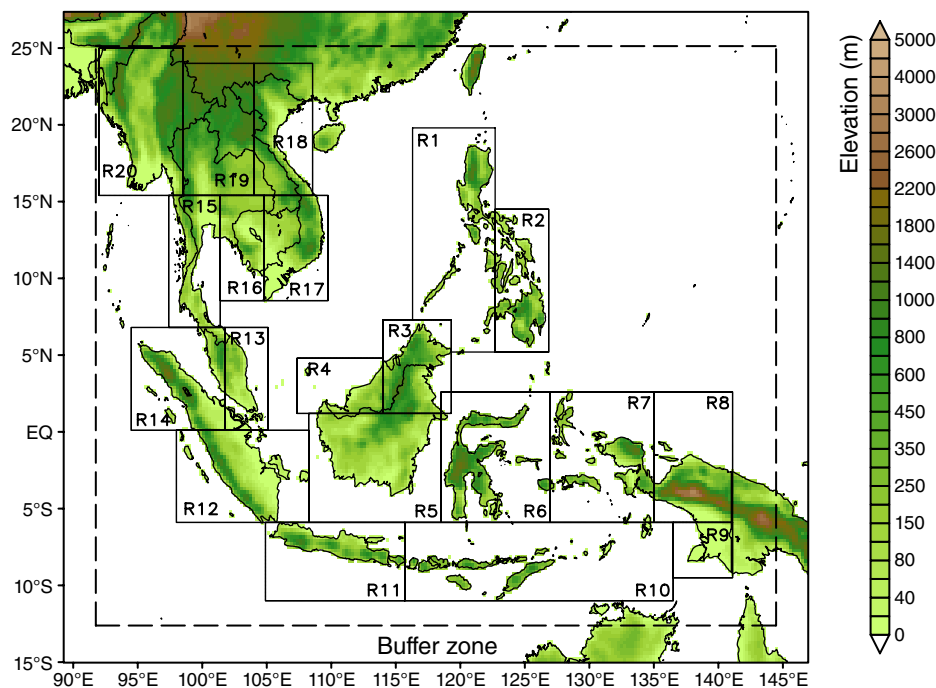


Figure 1. The simulation domain of SEACLID/CORDEX-SEA for the Southeast Asia region. The dashed box indicates the buffer zone of the simulation, while the boxes are the 20 sub-regions divisions (Juneng *et al.*, 2016). The shades represent the topography configuration in the model. [Colour figure can be viewed at wileyonlinelibrary.com].

study for validation against the simulated convective rain and large-scale precipitation.

3. Results and discussion

3.1. Precipitation climatology

The SEA seasonal precipitation climatology spatial pattern described by the observation datasets (only APHRODITE and TRMM are displayed) and simulations are shown in Figure 2. Generally, the equatorial region of SEA is wet while the SEA mainland is dry. During DJF, this north–south, dry-wet gradient is strong, whereas during JJA, the SEA mainland is considerably wetter than the equatorial region. Both the BATS and CLM simulations were able to correctly reproduce these precipitation characteristics. However, both the simulations produced similarly pronounced precipitation over the mountainous areas in the maritime continent for both DJF and JJA. In contrast, this precipitation feature was not observed in all the observation datasets, possibly because of the uncertainties in the observation datasets due to the sparse rain gauge network over the maritime continent (As-syakur *et al.*, 2016). TRMM on the other hand, often underestimated the precipitation over mountainous areas in the tropical region (Berg *et al.*, 2006; Huffman *et al.*, 2007). Over the ocean, both the BATS and CLM simulations were able to capture the DJF and JJA precipitation well, although both simulations overestimated the precipitation band over the South China Sea during JJA (Figure 2).

The BATS simulation was observed to have systematically overestimated the amount of on-land precipitation

throughout the SEA for all seasons (Figure 3, only comparison with APHRODITE and TRMM are shown). Meanwhile, the sign of precipitation bias simulated by the CLM simulation was location- and season-dependent. The BATS simulation was substantially wetter than that of CLM; the difference in the magnitude of precipitation between the BATS and CLM simulations over the land ranged from ~ 1 to more than 12 mm day^{-1} . During DJF, the largest difference between the BATS and CLM simulations was located at the maritime continent where the amount of precipitation was high. During this season, the precipitation produced by the BATS simulation was $\sim 8 \text{ mm day}^{-1}$ higher than that of CLM. In contrast, over the SEA mainland area, the difference in the amount of precipitation produced by the BATS and CLM simulations was small, with BATS giving only $\sim 1 \text{ mm day}^{-1}$ higher than CLM. During JJA on the other hand, the largest difference between the simulations was found on the SEA mainland. The amount of precipitation simulated by the BATS simulation was $\sim 8 \text{ mm day}^{-1}$ higher than that of CLM. In contrast, over the maritime continent, the amount of precipitation simulated by the BATS simulation was $\sim 4 \text{ mm day}^{-1}$ higher. The results were thus in agreement with those of Kang *et al.* (2014) and Li *et al.* (2016) in terms of the fact that the CLM land-surface scheme reduces the amount of on-land precipitation simulated by RegCM4.

Over the ocean, both BATS and CLM showed similar precipitation biases pattern with respect to TRMM. However, in terms of magnitude, notable differences of between -4 to 4 mm day^{-1} in the precipitation amount simulated by BATS and CLM were observed in both the DJF and JJA seasons (Figure 3). During DJF, BATS

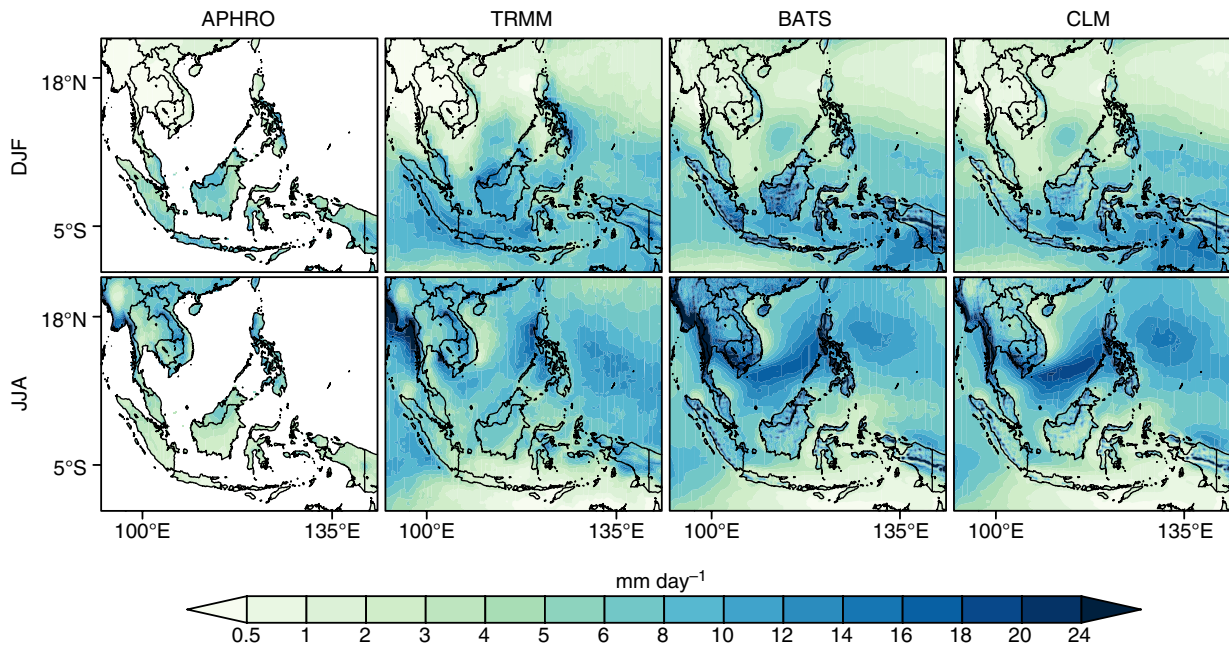


Figure 2. Daily mean precipitation seasonal climatology spatial pattern of APHRODITE, TRMM, BATS and CLM simulations for DJF and JJA. [Colour figure can be viewed at wileyonlinelibrary.com].

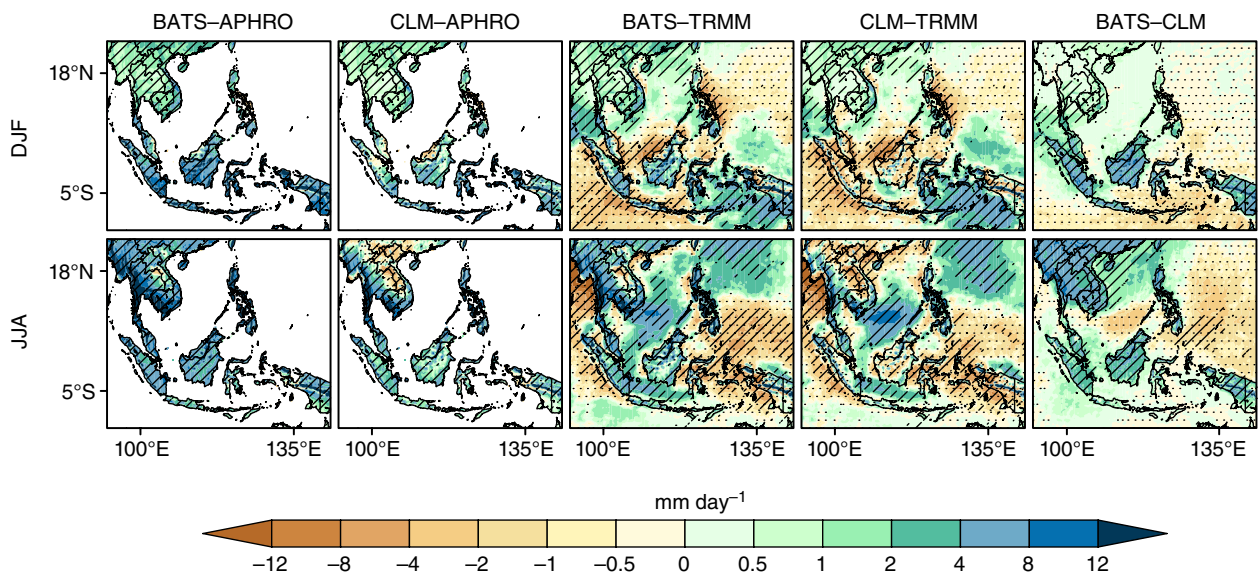


Figure 3. Comparison between the precipitation from BATS with APHRODITE, CLM with APHRODITE, BATS with TRMM, CLM with TRMM and BATS with CLM for DJF and JJA. Hatches indicate that the comparison is significant at a significance level of 0.05 using the Student's *t*-test. The negative values were overlaid with dots. [Colour figure can be viewed at wileyonlinelibrary.com].

simulated slightly more precipitation ($\sim 2 \text{ mm day}^{-1}$) than CLM over the upper portion of the eastern tropical Indian Ocean (TIO) and South China Sea (SCS), and slightly less ($\sim 2 \text{ mm day}^{-1}$) over the western tropical Pacific Ocean (TPO) and lower portion of the eastern TIO. During JJA, the precipitation amount was higher ($\sim 4 \text{ mm day}^{-1}$) in BATS than CLM over the upper and lower portion of SCS as well as over eastern TIO. Over the central SCS and western TPO, CLM gave a higher precipitation amount ($\sim 4 \text{ mm day}^{-1}$) than BATS. However, the differences in precipitation between BATS and CLM over the ocean were largely not statistically significant.

Further statistical analysis was carried out on the simulated on-land precipitation climatology during DJF and JJA to compare the ability of each simulation to reproduce the precipitation spatial pattern (Figure 4). The results show that in terms of spatial agreement, both BATS and CLM simulations produced similar spatial correlation coefficients with respect to APHRODITE and TRMM during DJF (~ 0.61 for BATS, ~ 0.58 for CLM) and JJA (~ 0.39 for BATS, ~ 0.38 for CLM). This suggests that although the BATS simulation tends to overestimate the amount of precipitation, its ability to reproduce the precipitation climatology spatial pattern is still comparable

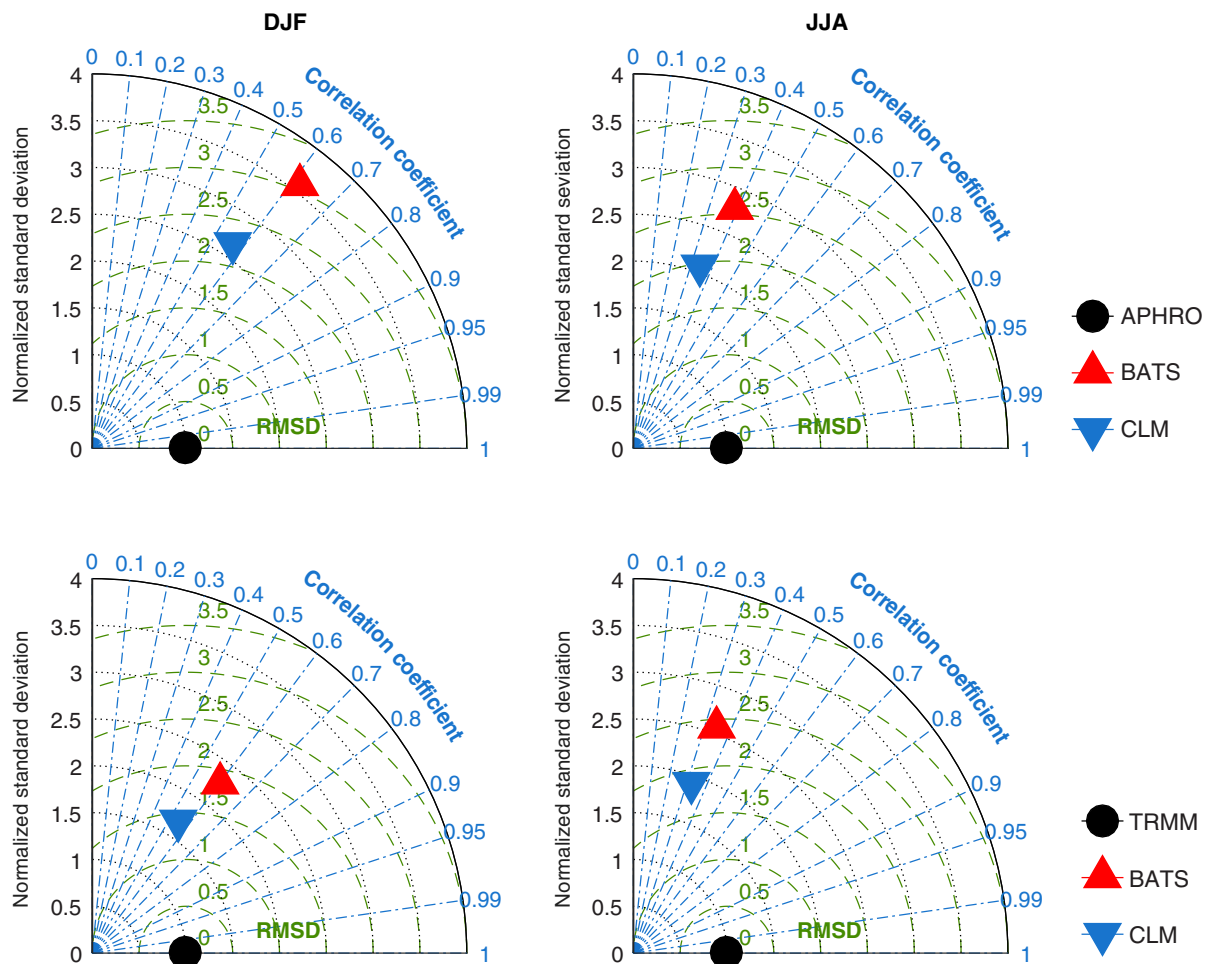


Figure 4. Taylor diagram providing various statistics for comparison of observations, BATS and CLM during DJF and JJA. The first row of the plots shows the comparison with APHRDITE, while the second row shows the comparison with TRMM. Only precipitation values over the land were used. [Colour figure can be viewed at wileyonlinelibrary.com].

with that of CLM. This finding is consistent with those of Tiwari *et al.* (2015) over the western Himalayas, where both the BATS and CLM were able to represent the seasonal mean precipitation distribution well. In addition, in terms of spatial root mean square difference (RMSD) and standard deviation with respect to the observation datasets, the spatial RMSD and standard deviation of the CLM simulation are consistently smaller than that of BATS. For comparison with APHRDITE (TRMM), the RMSD for CLM was $\sim 2.2 \text{ mm day}^{-1}$ ($\sim 1.4 \text{ mm day}^{-1}$) in DJF and $\sim 2.0 \text{ mm day}^{-1}$ ($\sim 1.8 \text{ mm day}^{-1}$) in JJA, while $\sim 3.0 \text{ mm day}^{-1}$ ($\sim 1.8 \text{ mm day}^{-1}$) in DJF and $\sim 2.6 \text{ mm day}^{-1}$ ($\sim 2.4 \text{ mm day}^{-1}$) in JJA for BATS. This evidence shows that the amount of precipitation simulated by the CLM simulation is closer to that of the observation datasets compared with that of BATS, agreeing with other past studies conducted (e.g. Steiner *et al.*, 2005; Diro *et al.*, 2012; Kang *et al.*, 2014; Reboita *et al.*, 2014; Tiwari *et al.*, 2015; Wang *et al.*, 2015; Gao *et al.*, 2016; Li *et al.*, 2016).

3.2. Frequency of precipitation events

Further understanding of how the land-surface scheme influences the simulated precipitation requires additional

analysis. Here, we considered the frequencies of the precipitation events triggered by both BATS and CLM simulations, which were computed using the simulated daily precipitation. The occurrence of a precipitation event was defined as when the daily precipitation amount was at least 1.0 mm day^{-1} (e.g. Endo *et al.*, 2009; Kang *et al.*, 2014). For this assessment, daily TRMM precipitation data were used as validation data despite spanning a relatively short period (from year 1998 to 2007) compared with other observational datasets. The rationale for preferring TRMM is that the CRU and GPCP datasets only encompass the monthly value of precipitation, while the rain gauge data used to construct APHRDITE was scarce over the maritime continent (Yatagai *et al.*, 2009) and often shows lower precipitation over the equatorial regions (Juneng *et al.*, 2016). The observation-simulation comparison was carried out seasonally for the years 1998 to 2007. For meaningful comparisons of precipitation events across the seasons, we computed the ratio (in percentages) of precipitation events to the total number of simulated days in a season (Figure 5).

Figure 5 shows that both BATS and CLM strongly overestimated the number of precipitation events throughout

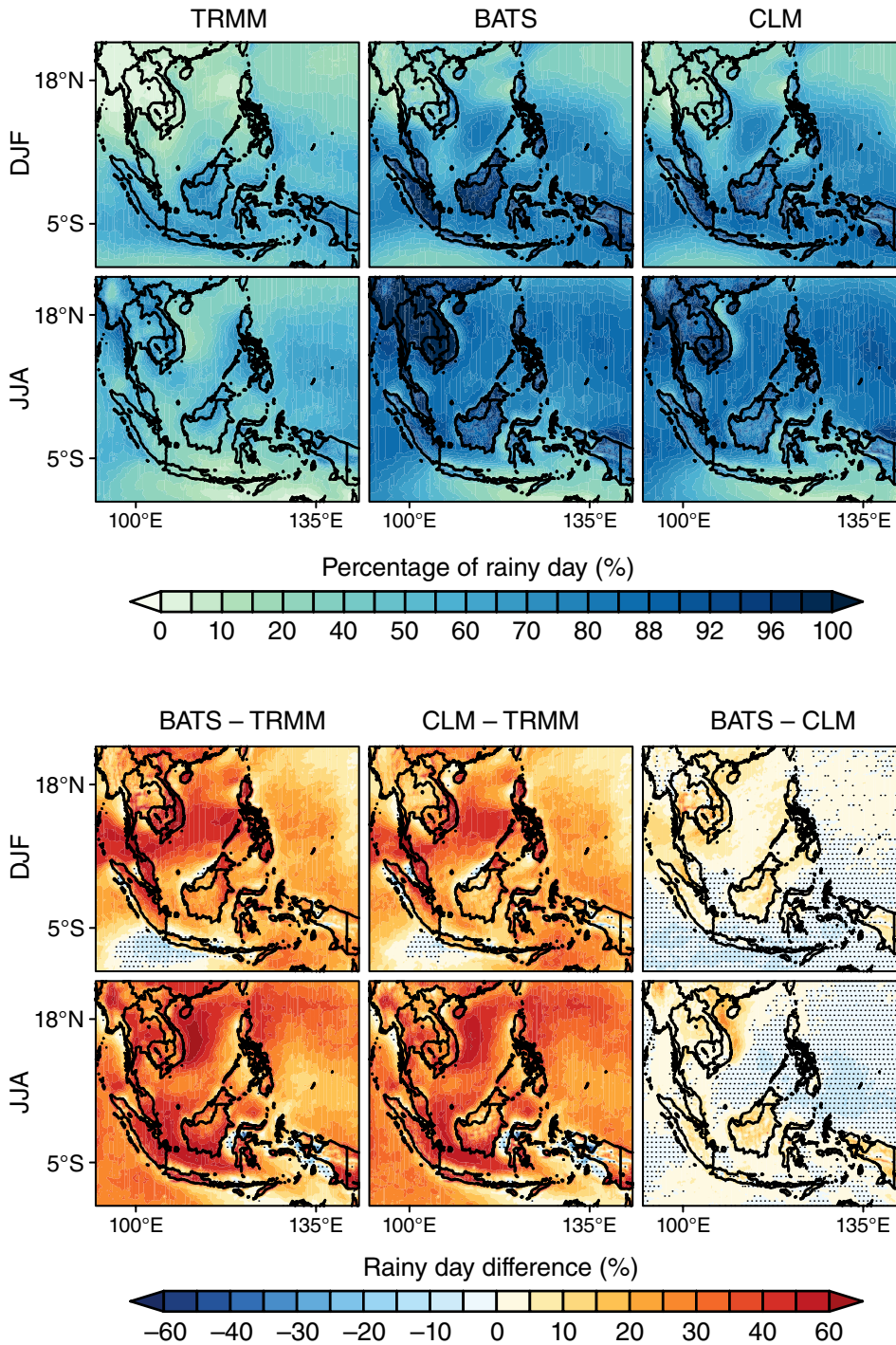


Figure 5. Seasonal percentage of precipitation events in TRMM, BATS and CLM for the years 1998 to 2007 in DJF and JJA (upper panel), and the differences in the precipitation events from BATS with TRMM, CLM with TRMM and BATS with CLM (lower panel). The negative values were overlaid with dots. [Colour figure can be viewed at wileyonlinelibrary.com].

the period; this overestimation can reach more than 50% with respect to TRMM (Figure 5). Furthermore, the overestimation of the frequency of precipitation events by both simulations occurred regardless of the season; however, the magnitude of this overestimation varied with season and location. During DJF, the precipitation event frequency produced by both simulations over the maritime continent was notably overestimated. However, the simulated frequency of precipitation events closely resembled

that of TRMM over the SEA mainland. During JJA, the strongest overestimation of precipitation event frequency occurred over the SEA mainland. Nevertheless, both BATS and CLM reasonably reproduced the north–south contrast of the frequency of the precipitation event. There was also a pronounced difference between the degrees of overestimation between the two simulations. CLM consistently produced a smaller overestimation of on-land precipitation compared with BATS. The difference between the on-land

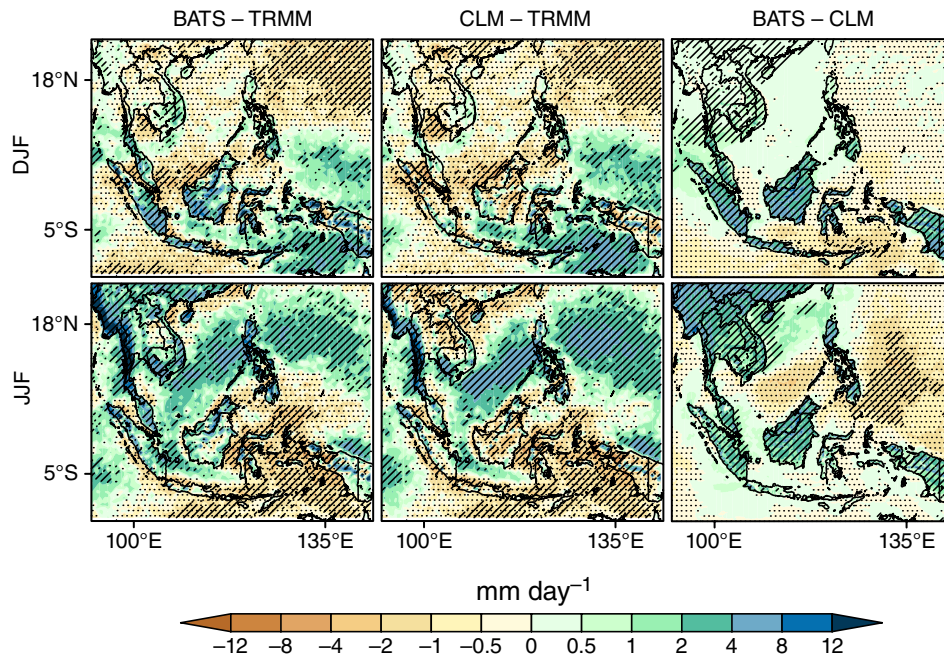


Figure 6. Comparison of seasonal convective precipitation (CPr) climatological mean between BATS and TRMM, CLM and TRMM, and BATS and CLM for DJF and JJA. Hatches indicate that the comparison is significant at a significance level of 0.05 using Student's *t*-test. The negative values were overlaid with dots. [Colour figure can be viewed at wileyonlinelibrary.com].

precipitation event frequencies simulated by the two simulations was sometimes as large as $\sim 20\%$. This evidence shows that in addition to reducing the amount of simulated on-land precipitation, the CLM land-surface scheme was also able to reduce the frequency of precipitation, consistent with the findings of Kang *et al.* (2014) over the East Asia region. During DJF, the precipitation frequency over the ocean in BATS and CLM showed marginal difference to that over land. During JJA, however, the precipitation frequency over northern SCS was slightly higher ($\sim 10\%$) in BATS. Over the central SCS and western TPO, precipitation frequency was slightly higher ($\sim 10\%$) in CLM than in BATS. Notably, the spatial pattern of the differences in precipitation frequency from BATS and CLM over the ocean (Figure 5) corresponds well to the difference in the oceanic precipitation amount (Figure 3).

3.3. Convective and large-scale precipitation

The CPr plays an important role in the production of total precipitation over SEA (e.g. Ngo-Duc *et al.*, 2017) especially over the maritime continent; this is a highly convective active region as it is surrounded by a warm ocean with complex topography (Ichikawa and Yasunari, 2006). Therefore, we carried out further analysis to assess the ability of BATS and CLM to reproduce CPr and large-scale precipitation (LPr). Comparing the simulated CPr between 1998 and 2007 with that produced by TRMM 3A25 (Figure 6), it is noticeable that the CLM simulation consistently underestimates the magnitude of CPr at the northern part of the SEA region, with a dry bias of up to 2 mm day^{-1} , depending on the season. The underestimation of the CPr in this region also occurred in the BATS simulation, except during the JJA season, where the

simulation tended to overestimate the actual magnitude of CPr. Over the maritime continent, the BATS simulation had a tendency to overestimate the amount of CPr, with wet bias ranging from $\sim 2 \text{ mm day}^{-1}$ to more than 12 mm day^{-1} . Over Southern Thailand and central Vietnam, both simulations consistently overestimated the magnitude of CPr.

The results also show that the magnitude of the on-land CPr produced by CLM simulation was smaller over the SEA region (Figure 6). The difference between the simulated CPrs ranged from $\sim 1 \text{ mm day}^{-1}$ to more than 8 mm day^{-1} , but was less than 12 mm day^{-1} , depending on the location and seasons. The difference in magnitude of the CPr generated by the BATS and CLM simulations was large when the precipitation was more dominated by CPr and vice versa. The CPr climatology spatial pattern difference between BATS and CLM simulation over SEA resembles to that of total precipitation (Figure 3) for all seasons. This resemblance shows that the precipitation simulated over SEA is very much influenced by the CPr. This result was consistent with those of Schumacher and Houze (2003), which reported that LPr was markedly lower over the maritime continent. Over the ocean, the difference in the CPr simulated by BATS and CLM was minimal, i.e. between -2 and 2 mm day^{-1} for DJF and JJA. Also, the spatial differences in the oceanic CPr climatology simulated by BATS and CLM were similar to that of total precipitation, and were mostly not statistically significant. Furthermore, the CPr over the ocean simulated by BATS and CLM showed a similar spatial pattern of biases with respect to TRMM for both DJF and JJA (Figure 6). Thus, the choice of land-surface scheme had no strong influence over the simulation of oceanic CPr.

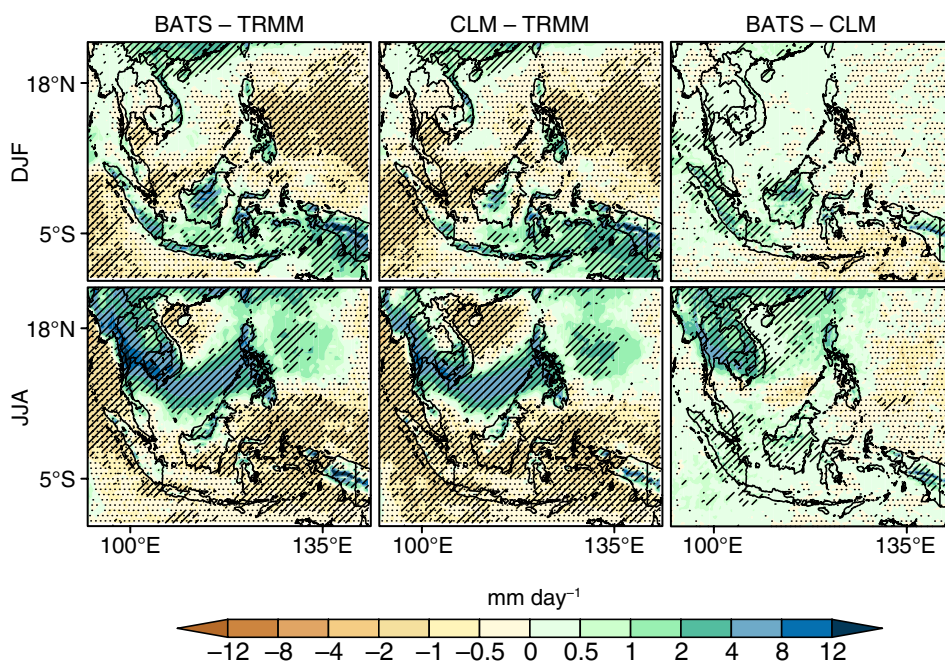


Figure 7. Comparison of seasonal large-scale precipitation (LPr) climatological mean between BATS and TRMM, CLM and TRMM, and BATS and CLM for DJF and JJA. Hatches indicate that the comparison is significant at a significance level of 0.05 using Student's *t*-test. The negative values were overlaid with dots. [Colour figure can be viewed at wileyonlinelibrary.com].

Over the East Asia region, Kang *et al.* (2014) suggested that the BATS land-surface scheme suppressed the formation of LPr due to the frequent generation of strong CPr. However, over the SEA region, the suppression of LPr by the BATS land-surface scheme was not observed in this study. The BATS and CLM LPr climatological bias spatial patterns with respect to TRMM are shown in Figure 7. Notably, both simulations produced similar bias patterns except during JJA, where the BATS simulation overestimated the LPr climatological mean over the whole SEA mainland. Overall, the LPr of BATS slightly exceeded that of the CLM with differences of between $\sim \pm 0$ to $\sim 1 \text{ mm day}^{-1}$ for DJF. During JJA, the LPr simulated by the BATS simulation was $\sim 4 \text{ mm day}^{-1}$ wetter than CLM over the SEA mainland. Generally, the results suggest that the choice of land-surface scheme has only a minimal impact on the formation of SEA LPr in the simulation. The difference between the results of this study and those of Kang *et al.* (2014) may be due to the precipitation over SEA being predominantly CPr. This can clearly be seen from Figure 8 which shows the percentage frequency of the occurrence of CPr and LPr with a daily amount $> 1 \text{ mm day}^{-1}$ to the total number of days simulated in each of the seasons from 1998 to 2007. The result in Figure 8 shows that the frequency of LPr in both BATS and CLM simulations was approximately the same throughout all the seasons (~ 5 to $\sim 30\%$), and was far smaller than CPr (from $\sim 10\%$ over the SEA mainland during DJF to $\sim 70\%$ lower). These findings were consistent with those of Schumacher and Houze (2003) in which over the tropics, the production of LPr is not as dependent on the strength of CPr. Therefore, the impact of the choice of land-surface scheme on the SEA LPr was not as significant

as reported by Kang *et al.* (2014) over the East Asia region.

3.4. Precipitation annual cycle and interannual variability

The assessments carried out so far show the ability of the CLM land-surface scheme to curb the over-intense and over-frequent precipitation in RegCM4 compared with the BATS scheme. Hence, the results thus far appear to show the advantages of the CLM scheme. However, it is also important to ensure that the CLM simulation is able to correctly simulate the most basic precipitation variabilities. Therefore, in this section the ability of the simulations to capture the on-land precipitation annual cycle and interannual precipitation between the years 1990 to 2007 is further examined.

The on-land precipitation annual cycles simulated by the BATS and CLM were examined by calculating the area-averaged precipitation of each of the 20 sub-regions shown in Figure 1. We avoided calculating the annual cycle of mean precipitation of the entire domain, as the climate type in SEA is not homogenous throughout the region (Siew *et al.*, 2014). Both the BATS and CLM simulated precipitation annual cycles show good agreement with the observations over most of the sub-regions (Figure 9). Compared with BATS, the magnitude of the annual cycle simulated by CLM is slightly closer to the range of observations over some sub-regions (e.g. R01–02, R10–11). This outcome could be expected as CLM produced less intense precipitation compared with BATS. However, the CLM simulation did not improve those annual cycles which were weakly simulated in BATS (e.g. R03–05, R12–14). The impact of the choice of land-surface scheme

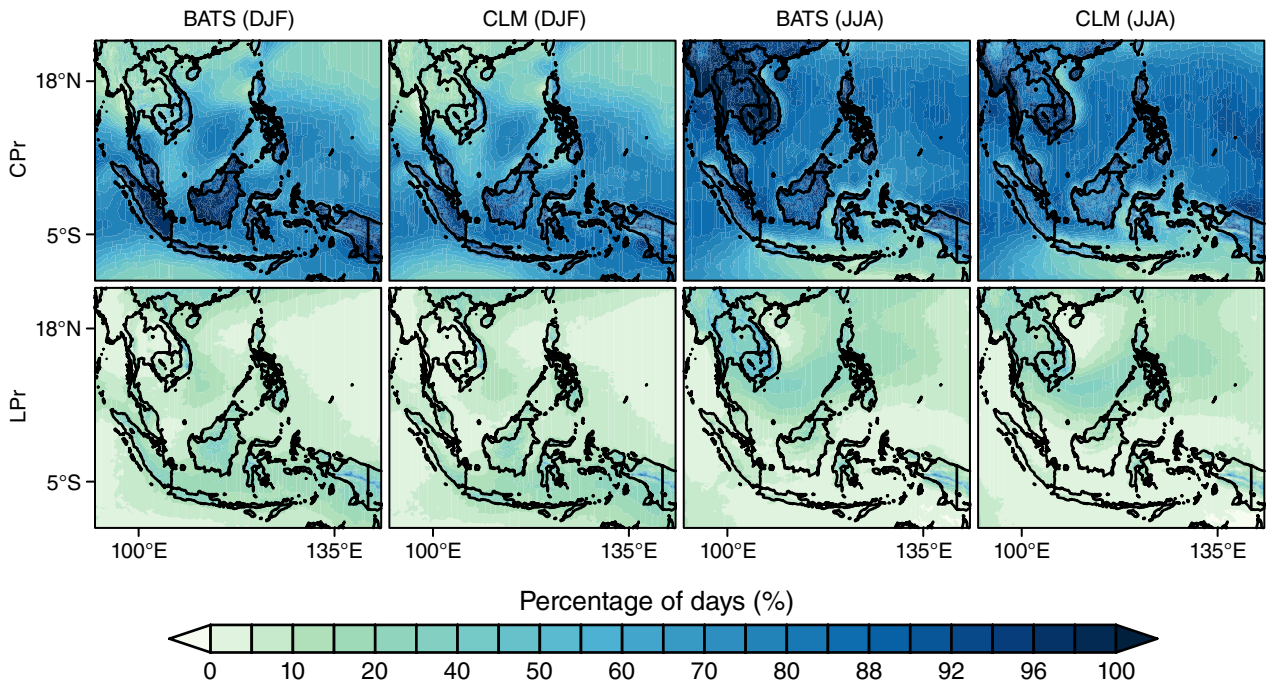


Figure 8. Seasonal percentage of CPr and LPr events in BATS and CLM for the years 1998 to 2007. [Colour figure can be viewed at wileyonlinelibrary.com].

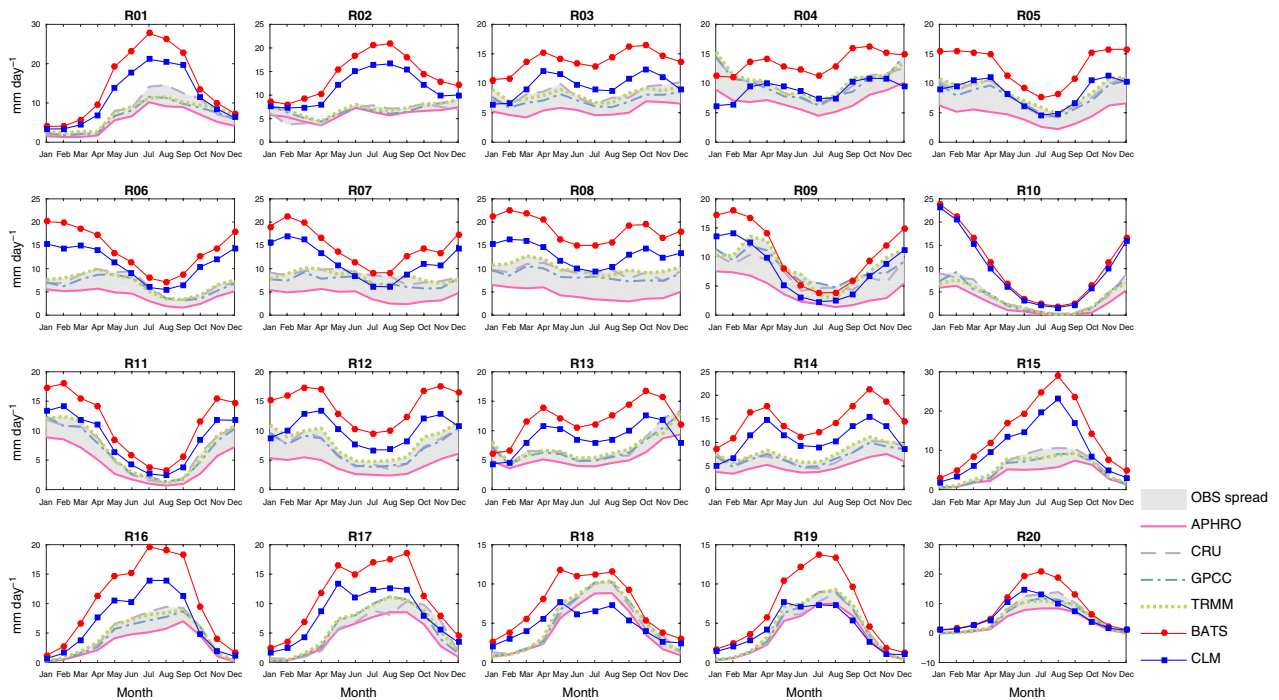


Figure 9. Annual cycles of the 20 sub-regions. The shaded area represents the spread of the observations; the solid, dashed, dashed dotted and dotted lines represent APHRODITE, CRU, GPCC and TRMM datasets, respectively. The round marker and square marker lines represent BATS and CLM, respectively. [Colour figure can be viewed at wileyonlinelibrary.com].

appears not to be as large as changing the choice of CPS from one to another as shown by Juneng *et al.* (2016). The impact that the choice of land-surface scheme had on the annual cycle was constrained to the magnitude of the cycle, as the CLM has been repeatedly shown to produce less precipitation compared with BATS.

Changing the land-surface scheme from BATS to CLM also does not appear to change the strength of the precipitation interannual variability and time evolution of the year-to-year seasonal precipitation simulation. Figure 10 shows the coefficient of variation of the seasonal mean rainfall for TRMM, BATS and CLM simulation. Although

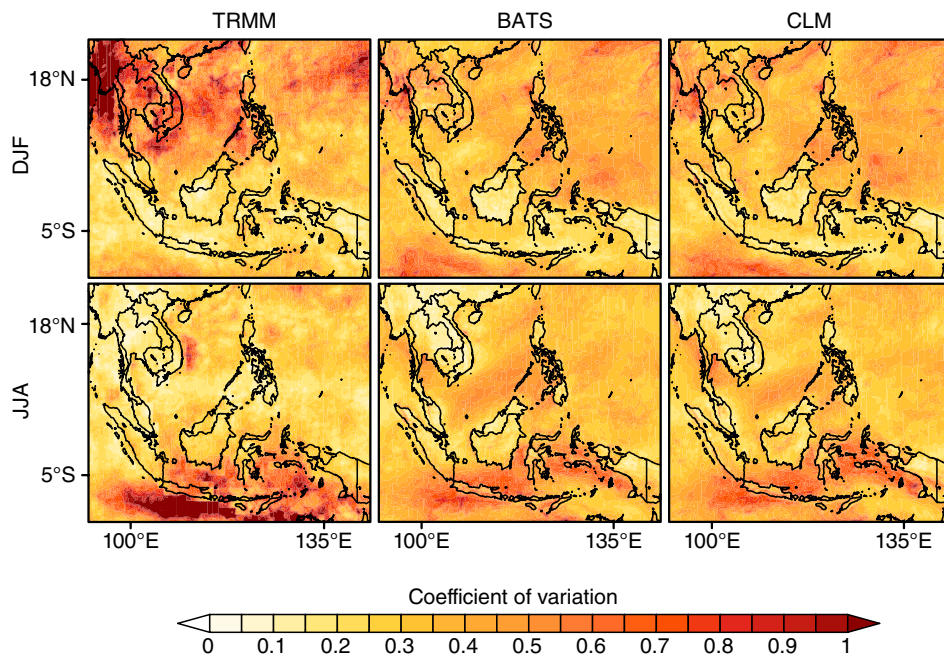


Figure 10. Precipitation coefficient of variation depicted by TRMM, BATS and CLM for DJF and JJA. [Colour figure can be viewed at wileyonlinelibrary.com].

both the simulations underestimated the strength of the variability over the western side of the SEA mainland during DJF ($\sim 20\%$ to $\sim 50\%$ weaker) and the southern region of SEA during JJA ($\sim 20\%$ to $\sim 50\%$ weaker), the strength of the variability simulated is overall closer to that of TRMM. Similarly, the spatial distribution of the seasonal mean precipitation coefficient of variation of BATS and CLM greatly resembles that of TRMM. This is in agreement with Fuentes-Franco *et al.* (2014) where it was found that there is a reasonable agreement between the model and observation in terms of the precipitation interannual variability.

To investigate the ability of BATS and CLM to reproducing the seasonal year-to-year precipitation variation, a grid-to-grid correlation was carried out on the seasonal mean precipitation between the simulations and observations (Figure 11; only the comparison with APHRODITE and TRMM are shown). Generally, both BATS and CLM were able to reproduce the year-to-year variation in precipitation reasonably well during DJF, except over certain parts of the maritime continent where the correlation coefficients were negative. During JJA, both simulations consistently produced negative year-to-year correlations over the SEA mainland with respect to observations (both APHRODITE and TRMM). Juneng *et al.* (2016) explained that this negative correlation can be related to the lack of air–sea coupling in both simulations. The study noticed that while the observed precipitation over the SEA mainland corresponded positively to the local heat fluxes and negatively to the sea surface temperature over the adjacent seas, the opposite was true for the simulated precipitation. Hence, the observed precipitation over the SEA mainland was largely locally forced but the simulated rainfall was dominated by the oceanic forcing

(Juneng *et al.*, 2016). The lack of air–sea coupling in the model resulted in the inability of the model to cool the sea surface temperature in the adjacent seas, thus unable to dampen the influence of oceanic forcing in the simulation (Juneng *et al.*, 2016). Nevertheless, it is clear from the result that choice of land-surface scheme does not seem to have any significant effect on the underlying dynamics governing the interannual variability in the model. Such an outcome may be expected as the precipitation interannual variability is modulated by large-scale phenomena such as El Niño–Southern Oscillation (e.g. Kripalani and Kulkarni, 1997; Tangang and Juneng, 2004; Juneng and Tangang, 2005; Salimun *et al.*, 2014).

3.5. Land-surface scheme and precipitation processes

The results in previous sections show that the behaviour of RegCM4 with MIT-Emanuel CPS in simulating the SEA precipitation amount and frequency was different when different land-surface schemes were coupled to the model. These differences in response can be attributed to the differences in soil moisture simulated in the model by BATS and CLM. Moreover, the inter-relationship and feedbacks between the soil moisture and precipitation has been widely discussed in various studies (e.g. Findell and Eltahir, 1997; Eltahir, 1998; Schär *et al.*, 1999). The soil moisture content in the simulation, released through latent heat, affects the simulated precipitation and vice versa. In conjunction with the overestimation of on-land precipitation in the BATS simulation, the overall surface soil moisture and latent heat flux in the BATS simulation over SEA was shown to be higher than that of CLM in terms of seasonal climatology (Figure 12). The overestimation of the surface soil moisture and hence latent heat flux in BATS compared with that of CLM was not unique to the SEA

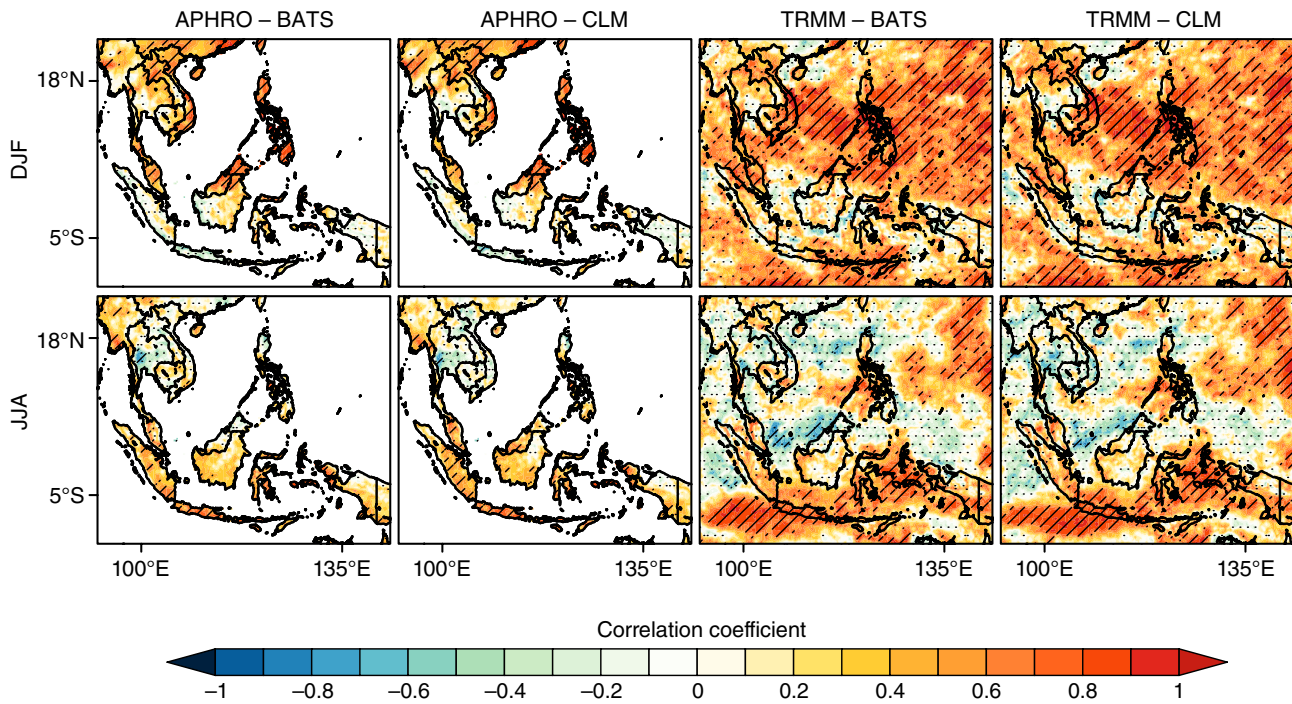


Figure 11. Point-to-point yearly seasonal mean rainfall correlation coefficient calculated between BATS and APHRODITE, CLM and APHRODITE, BATS and TRMM, and CLM and TRMM. Hatches indicate that the correlation coefficient is significant at a significance level of 0.05 using Student's *t*-test. The negative values were overlaid with dots. [Colour figure can be viewed at wileyonlinelibrary.com].

region, as this overestimation has been reported over other simulated domains (e.g. Dai *et al.*, 2003; Kang *et al.*, 2014; Li *et al.*, 2016). The lack of soil moisture in CLM can be attributed to its more detailed soil texture boundary condition in conjunction with its hydrological treatment of the soil column (Steiner *et al.*, 2009), while the overestimation of soil moisture in BATS is largely due to the uncertainty of the prescribed soil properties (Kang *et al.*, 2014).

The linkage between soil moisture, latent heat flux and precipitation while present, is not always direct. During DJF, the surface soil moisture and latent heat flux simulated by BATS were shown to be much higher than that of CLM for the southern part of SEA mainland. However, the amount of precipitation generated by the two simulations was closely comparable and did not reflect these differences. This shortcoming is very likely due to the dependency of the soil moisture-precipitation linkage on the activeness of convective activities, and during DJF, the convective activities over the SEA mainland are minimal. To examine this issue, the seasonal mean convective available potential energy (CAPE) and convective inhibition (CIN) were calculated at the lowest level in the BATS and CLM simulations. The CAPE and CIN were calculated using the daily mean vertical atmospheric data over the land area for the 20 sub-regions defined above (Figure 13).

The estimated CAPE and CIN results indicate that the convective activities on land showed strong seasonality over the SEA mainland (R15 to 20) and Philippines (R01 and 02). During DJF, both simulations show the smallest CAPE over these regions, signifying the convective

inactivity. In contrast, CAPE was large during JJA. The responses of the soil moisture-precipitation feedback to the seasonality of the convective activities in SEA can be seen from the differences in the CAPE and CIN between BATS and CLM. The comparison showed a similar and comparable magnitude of CAPE between BATS and CLM during DJF. However, during JJA, the magnitude of CAPE in the BATS was larger than that of CLM. Hence, this comparison suggests that the influence that soil moisture has on the precipitation is actually dependent on the availability of the convective activities over the region.

Soil moisture influences the formation of CPR via the release of latent heat flux; higher surface soil moisture will release a higher content of latent heat flux, humidifying the lower atmosphere and reducing the height of the mixing level. This feedback causes the CAPE to increase and the CIN to decrease, allowing a higher amount of CPR to be formed. This high amount of precipitation formed later contributes to the higher amount of surface soil moisture content, forming a strong positive feedback loop. This is the case when coupling MIT-Emanuel to BATS. Coupling the drier CLM with MIT-Emanuel on the other hand, discourages the formation of such feedback. This is due to the ability of the precipitated water to easily infiltrate the soil column of CLM and hence is less likely to be stored in the soil (Steiner *et al.*, 2009). Thus, the soil moisture in CLM was lesser than BATS (Figure 12), reducing the amount of surface moisture which can be fed to the atmosphere. Consequently, the CAPE in CLM was lower while the CIN was higher (Figure 13), signifying that CPR was less likely to be formed in the CLM. The difficulty of CPR formation in CLM later discouraged the formation of strong

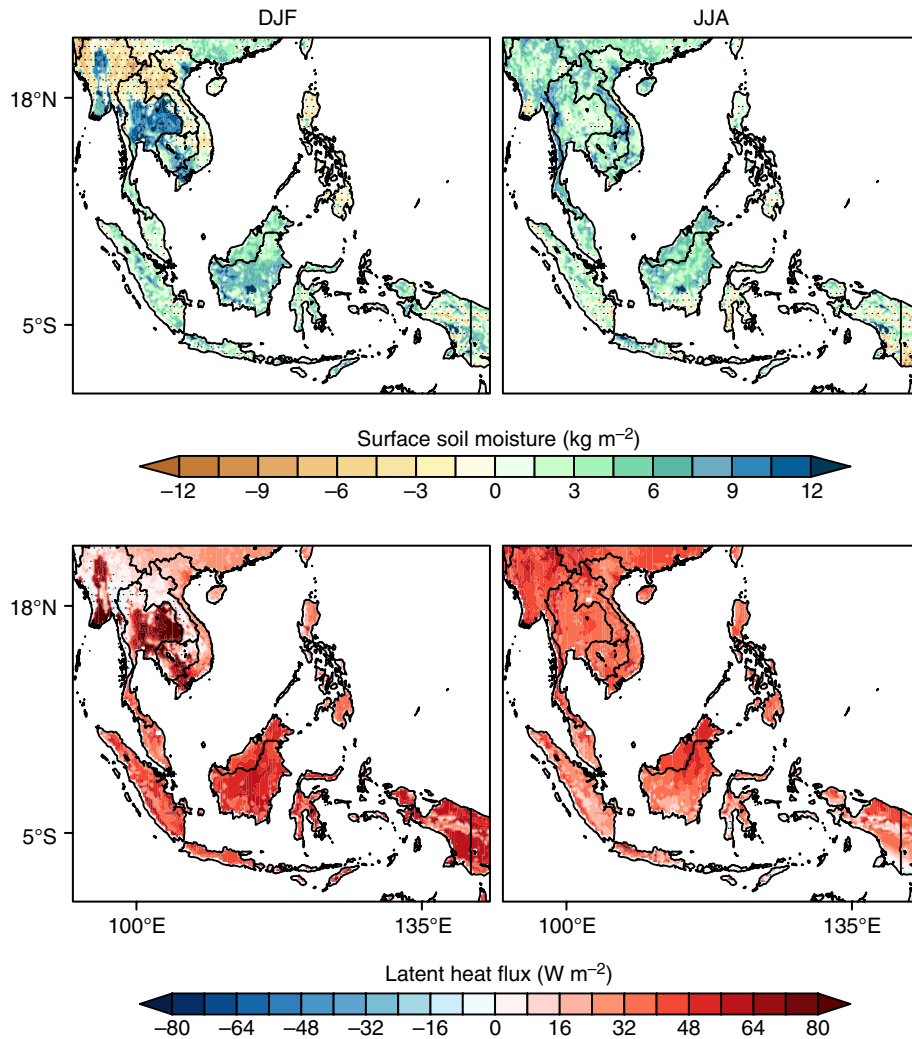


Figure 12. Surface soil moisture (upper panel) and latent heat flux (lower panel) seasonal climatology differences between BATS and CLM for DJF, and JJA. The negative values were overlaid with dots. [Colour figure can be viewed at wileyonlinelibrary.com].

positive soil moisture-precipitation feedback, thus resulting it showing a lower precipitation amount compared with BATS but closer to that of observations (Figure 4). Therefore, changing the land-surface scheme from BATS1e to CLM version 4.5 is recommended.

A comparison between the precipitation simulated by BATS and CLM (Figure 3) in the previous section shows that the oceanic precipitation in SEA was also affected by the change in the land-surface scheme, although to a much lesser extent than over land and was not significant. Nevertheless, this difference shows that the effect of soil moisture content on the precipitation was not confined to over land but took place over the ocean as well (e.g. Lofgren, 1995; Cook *et al.*, 2006). However, the role of soil moisture in this context could not have been direct. Rather, the soil moisture impacted the oceanic precipitation remotely by modifying the mesoscale circulation (e.g. Yan and Anthes, 1988). The interaction between soil moisture and mesoscale circulation can be observed from the mean sea level pressure (MSLP) and low level (1000 to 850 hPa) integrated moisture flux transport differences simulated by BATS and CLM (Figure 14).

The comparison between the MSLP simulated by BATS and CLM shows that the largest and most distinctive difference in MSLP was located over the SEA mainland (Figure 14). The influence of soil moisture on the MSLP, while present, was not constant but varied with the seasons. Despite BATS constantly producing higher soil moisture (Figure 12), its MSLP over the SEA mainland was higher during DJF but lower during JJA compared with that of CLM (Figure 14). This situation can be related to the amount of heat that the SEA mainland receives seasonally. During DJF, the SEA mainland was experiencing a winter climate, in which the heat flux was limited. The high soil moisture in BATS over central Thailand and Myanmar would be likely to cause a stronger evaporative cooling, promoting a higher MSLP (~ 0.4 – 1.0 hPa) over the mainland region. Notably, the surface temperature simulated by BATS over central Thailand and Myanmar was much cooler (~ 1.8 – 2.4 °C) than that of CLM. Because the MSLP and soil moisture in BATS over the SEA mainland were higher, more moisture from the surface could be transported out of the region to the Bay of Bengal and Gulf of Thailand, resulting in more

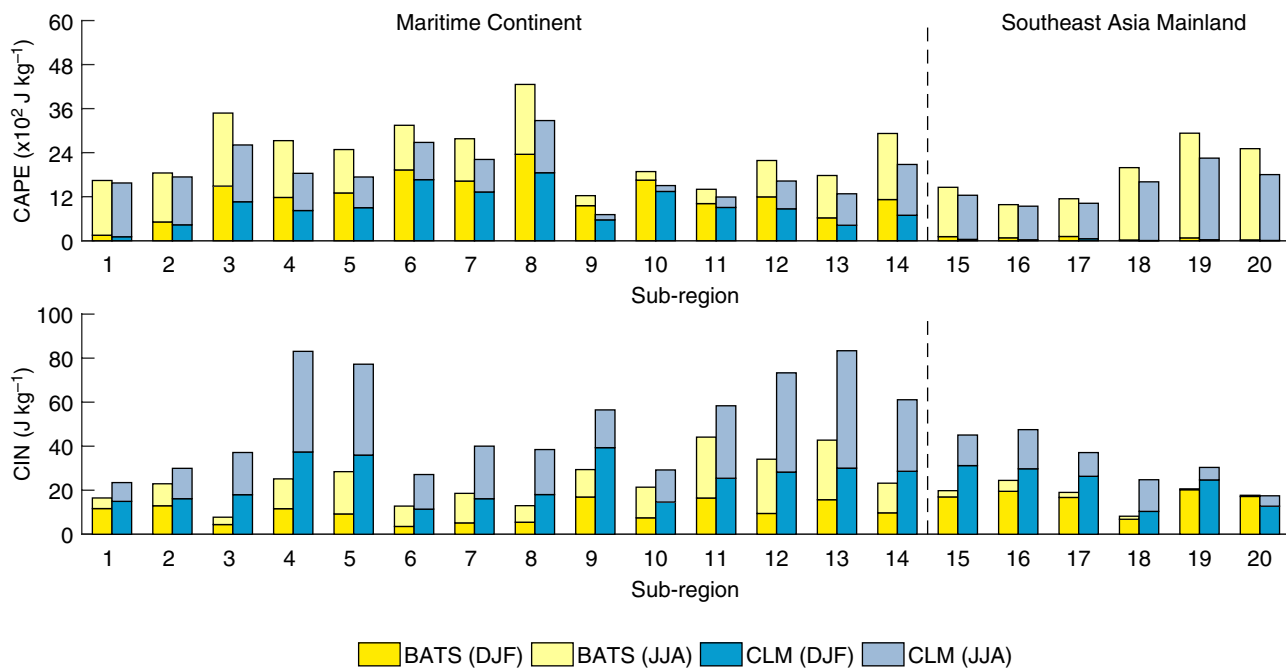


Figure 13. Seasonal mean CAPE (upper panel) and CIN (lower panel) at the atmospheric lowest level for 20 sub-regions in SEA. [Colour figure can be viewed at wileyonlinelibrary.com].

oceanic precipitation in BATS. In conjunction with the higher MSLP over the SEA mainland in BATS, several regions, including SCS and the lower portion of western TPO, experienced relatively low MSLP. However, over the eastern TIO and the upper portion of the western TPO, the MSLP were slightly higher. Hence, more moisture from the eastern tropical Indian Ocean (TIO) was transported to Sumatra, resulting in BATS showing less precipitation over the eastern TIO area compared with CLM, but more over the western coastal area of Sumatra (Figure 3).

During JJA on the other hand, the heat flux was higher over the SEA mainland as it was experiencing a summer climate. The high soil moisture in BATS would cause more latent heat to be released, producing a warmer environment. Thus, over the SEA mainland, the surface temperature simulated by BATS was generally warmer ($\sim 0.6\text{--}1.8^\circ\text{C}$) than that of CLM. This warmer environment in BATS over the SEA mainland would have resulted in a lower MSLP favouring the stronger south-westerly wind components in BATS. Hence, more moisture is transported from the eastern TIO and central SCS to the northern SCS passing through the SEA mainland causing more oceanic precipitation there. At the same time, the transportation of moisture through the SEA mainland could have resulted in more on-land LPr, explaining the difference in LPr observed between BATS and CLM over the mainland during JJA (Figure 7). The higher LPr in BATS caused the surface temperature over the Central Thailand to be slightly cooler ($\sim 0.6^\circ\text{C}$) than in CLM. In addition, in conjunction with the lower MSLP over the SEA mainland, BATS showed slightly higher MSLP over central SCS, western TPO and the lower portion of eastern TIO, although slightly lower MSLP over the other areas

compared with CLM. Hence, moisture from the western TPO was more likely to be transported westward in BATS than CLM, causing BATS to give lower oceanic precipitation over central SCS and western TPO than CLM.

4. Concluding remarks

In this study, the responses were analysed of the SEA precipitation seasonal spatial pattern, amount, frequency, annual cycle and interannual variability, as simulated by RegCM4, to a change in land-surface scheme from BATS version 1e to CLM version 4.5. For this purpose, two experiments were conducted for the period January 1989 to December 2007 using both BATS and CLM land-surface schemes using ERA-interim reanalysis as the model initial and boundary condition. As CPS MIT-Emanuel has been shown to produce the best precipitation simulation compared with other forms of CPS for SEA, it was used in both the experiments. All the other model configurations were kept the same. The output from the simulations was then compared with four different precipitation gridded products: APHRODITE, CRU, GPCC and TRMM.

Both BATS and CLM simulations reproduced the seasonal precipitation spatial pattern equally well. The spatial correlation coefficient between the simulated precipitation by BATS and CLM and that of observations were closely similar for all seasons. This can be attributed to the choice of CPS used. The main benefit in changing the land-surface scheme used in RegCM from BATS to CLM was the reduction in the magnitude and frequency of the on-land precipitation simulated. The largest reduction in the precipitation climatological mean simulated reached more than 12 mm day^{-1} , while the reduction in the

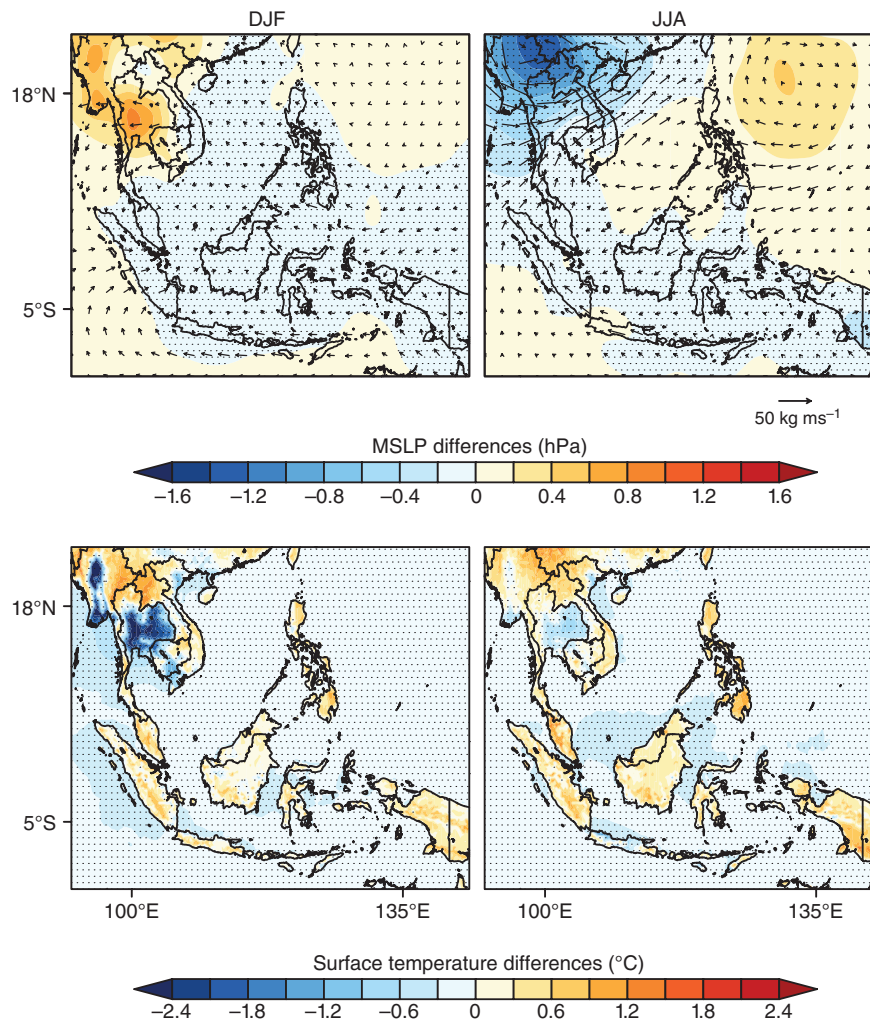


Figure 14. Comparison between the seasonal mean sea level pressure (MSLP), low level (1000–850 hPa) integrated moisture flux and surface temperature simulated by BATS and CLM during DJF and JJA. The negative values were overlaid with dots. [Colour figure can be viewed at wileyonlinelibrary.com].

frequency simulated reached more than 20%. Changing the land-surface scheme impacted the precipitation over the ocean, but the impact was not as large as that of over the land and had not affected the performance of the simulation in simulating ocean precipitation significantly in general. Attributed to the ability of CLM in preventing the model from over precipitation, its climatology spatial pattern had the smallest standard deviation and root mean square difference with respect to the observations.

Changing the land-surface scheme from BATS to CLM did not impact the precipitation annual cycle simulation as greatly as changing the CPS, as shown by Juneng *et al.* (2016) over SEA. However, changing the land-surface scheme to CLM did improve the magnitude of the annual cycles simulated. As CLM tends to reduce the precipitation bias simulated, the magnitude of the precipitation annual cycle simulated over all the 20 sub-regions by CLM were much closer to the observation range compared with BATS. The precipitation interannual variability simulated in SEA on the other hand was found to be insensitive to the choice of land-surface scheme used. This finding was very likely due to fact that the precipitation interannual

variability in SEA was modulated by large-scale phenomena (Kripalani and Kulkarni, 1997; Tangang and Juneng, 2004; Juneng and Tangang, 2005; Salimun *et al.*, 2014).

Land-surface scheme BATS was noticed to have consistently overestimated the surface soil moisture and latent heat flux compared with CLM. Such finding was consistent with previous studies. Consequently, the BATS simulation tended to generate more CPR as the CAPE was higher while the CIN was lower. Thus, a positive feedback loop between precipitation and soil moisture was created in the BATS simulation, contributing to the strong overestimation of precipitation amount and frequency. The differences in soil moisture of the two schemes also caused different responses in the MSLP over the SEA mainland. These differences in MSLP in turn promoted distinguishable regional atmospheric circulation and moisture flux transport, causing the oceanic precipitation as well as the LPr over the SEA mainland during JJA to differ between the two simulations.

Because the SEA is a convective active region and CLM could reduce the precipitation bias simulated when using the MIT-Emanuel CPS, this study recommends using the

CLM version 4.5 land-surface scheme for the simulation of SEA precipitation. However, it should be noted that the CLM simulation still over-estimate the frequency of the precipitation over the region. To further improve the precipitation simulations in SEA, future studies should examine two prospects. The first is the application of convection suppression in the simulation, because the application of various convection suppression criteria has been repeatedly shown to improve the precipitation simulation (e.g. Chow *et al.*, 2006; Zou and Zhou, 2013). The second area for future work is the fine tuning of the entrainment and detrainment rate in the CPS for SEA. The study conducted by Wang *et al.* (2007) showed that the development and strength of deep convection can be influenced by the entrainment/detrainment rate. Furthermore, studies showed that using a different data source for land cover can have significant impact on the simulation of climate over China (e.g. Yan and Xie, 2013; Han *et al.*, 2015). Given that BATS and CLM are use different sources of land cover, it will be important for future work to investigate how the use of different sources of land cover could impact climate simulations of SEA. In addition to precipitation, the ability of RegCM4 to simulate the surface temperature remains a concern. A systematic cold bias in SEA surface temperature simulated by RegCM4 using BATS1e land-surface scheme, regardless of the choice of CPS, has been reported by Ngo-Duc *et al.* (2017). Although Reboita *et al.* (2014) and Gao *et al.* (2016) showed that the MIT-Emanuel-CLM combination in RegCM could yield good results for surface temperature simulation over the South America and China region, our preliminary comparison (not shown) suggests that changing the land-surface scheme to CLM did not improve the cold bias over SEA. Therefore, it is recommended that a detailed future analysis of the response of surface temperature to the land-surface scheme in SEA should be conducted.

Acknowledgements

This research was funded by the Asia Pacific Network for Global Change Research (ARCP2013-17NMY-Tangang/ST-2013-017, ARCP2014-07CMY-Tangang/ST-2015-003, ARCP2015-04CMY-Tangang/ST-2015-003) and the Universiti Kebangsaan Malaysia ICONIC-2013-001. The authors would also like to acknowledge the Malaysian Ministry of Education for supporting this study through the MyBrain15 program.

References

- Arakawa A. 2004. The cumulus parameterization problem: past, present, and future. *J. Clim.* **17**(13): 2493–2525. [https://doi.org/10.1175/1520-0442\(2004\)017<2493:RATCPP>2.0.CO;2](https://doi.org/10.1175/1520-0442(2004)017<2493:RATCPP>2.0.CO;2).
- As-syakur AR, Osawa T, Miura F, Nuarsa IW, Ekayanti NW, Dharma IGBS, Adnyana IWS, Arthana IW, Tanaka T. 2016. Maritime continent rainfall variability during the TRMM era: the role of monsoon, topography and El Niño Modoki. *Dyn. Atmos. Oceans* **75**: 58–77. <https://doi.org/10.1016/j.dynatmoce.2016.05.004>.
- Berg W, L'Ecuyer T, Kummerow C. 2006. Rainfall climate regimes: the relationship of regional TRMM rainfall biases to the environment. *J. Appl. Meteorol. Climatol.* **45**(3): 434–454. <https://doi.org/10.1175/JAM2331.1>.
- Chow KC, Chan JCL, Pal JS, Giorgi F. 2006. Convection suppression criteria applied to the MIT cumulus parameterization scheme for simulating the Asian summer monsoon. *Geophys. Res. Lett.* **33**(24): L24709. <https://doi.org/10.1029/2006GL028026>.
- Cook BI, Bonan GB, Levis S. 2006. Soil moisture feedbacks to precipitation in Southern Africa. *J. Clim.* **19**(17): 4198–4206. <https://doi.org/10.1175/JCLI3856.1>.
- Cruz FT, Sasaki H, Narisma GT. 2016. Assessing the sensitivity of the non-hydrostatic regional climate model to boundary conditions and convective schemes over the Philippines. *J. Meteorol. Soc. Jpn.* **94A**: 165–179. <https://doi.org/10.2151/jmsj.2015-059>.
- Dai Y, Zeng X, Dickinson RE, Baker I, Bonan GB, Bosilovich MG, Denning AS, Dirmeyer PA, Houser PR, Niu G, Oleson KW, Schlosser CA, Yang Z-L. 2003. The common land model. *Bull. Am. Meteorol. Soc.* **84**(8): 1013–1023. <https://doi.org/10.1175/BAMS-84-8-1013>.
- Dee DP, Uppala SM, Simmons AJ, Berrisford P, Poli P, Kobayashi S, Andrae U, Balmaseda MA, Balsamo G, Bauer P, Bechtold P, Beljaars ACM, van de Berg L, Bidlot J, Bormann N, Delsol C, Dragani R, Fuentes M, Geer AJ, Haimberger L, Healy SB, Hersbach H, Hólm EV, Isaksen L, Kållberg P, Köhler M, Matricardi M, McNally AP, Monge-Sanz BM, Morcrette J-J, Park B-K, Peubey C, de Rosnay P, Tavolato C, Thépaut J-N, Vitart F. 2011. The ERA-Interim reanalysis: configuration and performance of the data assimilation system. *Q. J. R. Meteorol. Soc.* **137**(656): 553–597. <https://doi.org/10.1002/qj.828>.
- Dickinson E, Henderson-Sellers A, Kennedy J. 1993. Biosphere-Atmosphere Transfer Scheme (BATS) Version 1e as Coupled to the NCAR Community Climate Model. NCAR Technical Note NCAR/TN-387+STR. <https://doi.org/10.5065/D67W6959>.
- Diro G, Rauscher S, Giorgi F, Tompkins A. 2012. Sensitivity of seasonal climate and diurnal precipitation over Central America to land and sea surface schemes in RegCM4. *Clim. Res.* **52**(1): 31–48. <https://doi.org/10.3354/cr01049>.
- Eltahir EAB. 1998. A soil moisture–rainfall feedback mechanism: 1. Theory and observations. *Water Resour. Res.* **34**(4): 765. <https://doi.org/10.1029/97WR03499>.
- Emanuel KA, Živković-Rothman M. 1999. Development and evaluation of a convection scheme for use in climate models. *J. Atmos. Sci.* **56**(11): 1766–1782. [https://doi.org/10.1175/1520-0469\(1999\)056<1766:DAEOAC>2.0.CO;2](https://doi.org/10.1175/1520-0469(1999)056<1766:DAEOAC>2.0.CO;2).
- Emori S, Nozawa T, Numaguti A, Uno I. 2001. Importance of cumulus parameterization for precipitation simulation over East Asia in June. *J. Meteorol. Soc. Jpn.* **79**(4): 939–947. <https://doi.org/10.2151/jmsj.79.939>.
- Endo N, Matsumoto J, Lwin T. 2009. Trends in precipitation extremes over Southeast Asia. *SOLA* **5**: 168–171. <https://doi.org/10.2151/sola.2009-043>.
- Fekete BM, Vörösmarty CJ, Roads JO, Willmott CJ. 2004. Uncertainties in precipitation and their impacts on runoff estimates. *J. Clim.* **17**(2): 294–304. [https://doi.org/10.1175/1520-0442\(2004\)017<0294:UIPATI>2.0.CO;2](https://doi.org/10.1175/1520-0442(2004)017<0294:UIPATI>2.0.CO;2).
- Findell KL, Eltahir EAB. 1997. An analysis of the soil moisture-rainfall feedback, based on direct observations from Illinois. *Water Resour. Res.* **33**(4): 725–735. <https://doi.org/10.1029/96WR03756>.
- Francisco RV, Argete J, Giorgi F, Pal J, Bi X, Gutowski WJ. 2006. Regional model simulation of summer rainfall over the Philippines: effect of choice of driving fields and ocean flux schemes. *Theor. Appl. Climatol.* **86**(1–4): 215–227. <https://doi.org/10.1007/s00704-005-0216-2>.
- Fuentes-Franco R, Coppola E, Giorgi F, Graef F, Pavia EG. 2014. Assessment of RegCM4 simulated inter-annual variability and daily-scale statistics of temperature and precipitation over Mexico. *Clim. Dyn.* **42**(3–4): 629–647. <https://doi.org/10.1007/s00382-013-1686-z>.
- Gao X-J, Shi Y, Giorgi F. 2016. Comparison of convective parameterizations in RegCM4 experiments over China with CLM as the land surface model. *Atmos. Oceanic Sci. Lett.* **9**(4): 246–254. <https://doi.org/10.1080/16742834.2016.1172938>.
- Gianotti RL, Eltahir EAB. 2014a. Regional climate modeling over the maritime continent. Part I: new parameterization for convective cloud fraction. *J. Clim.* **27**(4): 1488–1503. <https://doi.org/10.1175/JCLI-D-13-00127.1>.
- Gianotti RL, Eltahir EAB. 2014b. Regional climate modeling over the maritime continent. Part II: new parameterization for autoconversion of convective rainfall. *J. Clim.* **27**(4): 1504–1523. <https://doi.org/10.1175/JCLI-D-13-00171.1>.

- Gianotti RL, Zhang D, Eltahir EAB. 2012. Assessment of the regional climate model version 3 over the maritime continent using different cumulus parameterization and land surface schemes. *J. Clim.* **25**(2): 638–656. <https://doi.org/10.1175/JCLI-D-11-00025.1>.
- Giorgi F, Coppola E, Solmon F, Mariotti L, Sylla M, Bi X, Elguindi N, Diro G, Nair V, Giuliani G, Turuncoglu U, Cozzini S, Guttler I, O'Brien T, Tawfik A, Shalaby A, Zakey A, Steiner A, Stordal F, Sloan L, Brankovic C. 2012. RegCM4: model description and preliminary tests over multiple CORDEX domains. *Clim. Res.* **52**(1): 7–29. <https://doi.org/10.3354/cr01018>.
- Giorgi F, Jones C, Asrar GR. 2009. Addressing climate information needs at the regional level: the CORDEX framework. *WMO Bull.* **58**(3): 175–183.
- Giorgi F, Marinucci MR, Bates GT. 1993. Development of a second-generation regional climate model (RegCM2). Part I: boundary-layer and radiative transfer processes. *Mon. Weather Rev.* **121**(10): 2794–2813. [https://doi.org/10.1175/1520-0493\(1993\)121<2794:DOASGR>2.0.CO;2](https://doi.org/10.1175/1520-0493(1993)121<2794:DOASGR>2.0.CO;2).
- Han Z, Gao X, Shi Y, Wu J, Wang M, Giorgi F. 2015. Development of Chinese high resolution land cover data for the RegCM4/CLM and its impact on regional climate simulation. *J. Glaciol. Geocryol.* **37**(4): 857–866. <https://doi.org/10.7522/j.issn.1000-0240.2015.0095>.
- Holtlag AAM, De Bruijn EIF, Pan H-L. 1990. A high resolution air mass transformation model for short-range weather forecasting. *Mon. Weather Rev.* **118**(8): 1561–1575. [https://doi.org/10.1175/1520-0493\(1990\)118<1561:AHRAMT>2.0.CO;2](https://doi.org/10.1175/1520-0493(1990)118<1561:AHRAMT>2.0.CO;2).
- Huffman GJ, Bolvin DT, Nelkin EJ, Wolff DB, Adler RF, Gu G, Hong Y, Bowman KP, Stocker EF. 2007. The TRMM multisatellite precipitation analysis (TMPA): quasi-global, multiyear, combined-sensor precipitation estimates at fine scales. *J. Hydrometeorol.* **8**(1): 38–55. <https://doi.org/10.1175/JHM560.1>.
- Ichikawa H, Yasunari T. 2006. Time–space characteristics of diurnal rainfall over Borneo and surrounding oceans as observed by TRMM-PR. *J. Clim.* **19**(7): 1238–1260. <https://doi.org/10.1175/JCLI3714.1>.
- Juneng L, Tangang F, Chung J, Ngai S, Tay T, Narisma G, Cruz F, Phan-Van T, Ngo-Duc T, Santisirisoombon J, Singhruck P, Gunawan D, Aldrian E. 2016. Sensitivity of Southeast Asia rainfall simulations to cumulus and air-sea flux parameterizations in RegCM4. *Clim. Res.* **69**(1): 59–77. <https://doi.org/10.3354/cr01386>.
- Juneng L, Tangang FT. 2005. Evolution of ENSO-related rainfall anomalies in Southeast Asia region and its relationship with atmosphere–ocean variations in Indo-Pacific sector. *Clim. Dyn.* **25**(4): 337–350. <https://doi.org/10.1007/s00382-005-0031-6>.
- Kalognomou E-A, Lennard C, Shongwe M, Pinto I, Favre A, Kent M, Hewitson B, Dosio A, Nikulin G, Panitz H-J, Büchner M. 2013. A diagnostic evaluation of precipitation in CORDEX models over Southern Africa. *J. Clim.* **26**(23): 9477–9506. <https://doi.org/10.1175/JCLI-D-12-00703.1>.
- Kang S, Im E-S, Ahn J-B. 2014. The impact of two land-surface schemes on the characteristics of summer precipitation over East Asia from the RegCM4 simulations. *Int. J. Climatol.* **34**(15): 3986–3997. <https://doi.org/10.1002/joc.3998>.
- Kripalani RH, Kulkarni A. 1997. Rainfall variability over South-east Asia – connections with Indian monsoon and ENSO extremes: new perspectives. *Int. J. Climatol.* **17**(11): 1155–1168. [https://doi.org/10.1002/\(SICI\)1097-0088\(199709\)17:11<1155::AID-JOC188>3.0.CO;2-B](https://doi.org/10.1002/(SICI)1097-0088(199709)17:11<1155::AID-JOC188>3.0.CO;2-B).
- Kwan MS, Tangang FT, Juneng L. 2014. Present-day regional climate simulation over Malaysia and western maritime continent region using PRECIS forced with ERA40 reanalysis. *Theor. Appl. Climatol.* **115**(1–2): 1–14. <https://doi.org/10.1007/s00704-013-0873-5>.
- Li Y-B, Tam C-Y, Huang W-R, Cheung KKW, Gao Z. 2016. Evaluating the impacts of cumulus, land surface and ocean surface schemes on summertime rainfall simulations over East-to-southeast Asia and the western north Pacific by RegCM4. *Clim. Dyn.* **46**(7–8): 2487–2505. <https://doi.org/10.1007/s00382-015-2714-y>.
- Lofgren BM. 1995. Sensitivity of land–ocean circulations, precipitation, and soil moisture to perturbed land surface albedo. *J. Clim.* **8**(10): 2521–2542. [https://doi.org/10.1175/1520-0442\(1995\)008<2521:SOLCPA>2.0.CO;2](https://doi.org/10.1175/1520-0442(1995)008<2521:SOLCPA>2.0.CO;2).
- Mitchell TD, Jones PD. 2005. An improved method of constructing a database of monthly climate observations and associated high-resolution grids. *Int. J. Climatol.* **25**(6): 693–712. <https://doi.org/10.1002/joc.1181>.
- Ngo-Duc T, Tangang FT, Santisirisoombon J, Cruz F, Trinh-Tuan L, Nguyen-Xuan T, Phan-Van T, Juneng L, Narisma G, Singhruck P, Gunawan D, Aldrian E. 2017. Performance evaluation of RegCM4 in simulating extreme rainfall and temperature indices over the CORDEX-Southeast Asia region. *Int. J. Climatol.* **37**: 1634–1647. <https://doi.org/10.1002/joc.4803>.
- Oleson KW, Dai Y, Bonan G, Mike B, Dickinson R, Dirmeyer P, Hoffman F, Houser P, Levis S, Niu G-Y, Thornton P, Vertenstein M, Yang Z-L, Zeng X. 2004. Technical description of the Community Land Model (CLM). NCAR Technical Note NCAR/TN-461+STR. <https://doi.org/10.5065/D6N877R0>.
- Oleson KW, Lawrence DM, Bonan GB, Drewniak B, Huang M, Charles DK, Levis S, Li F, Riley WJ, Subin ZM, Swenson SC, Thornton PE, Bozbiyik A, Fisher R, Heald CL, Kluzek E, Lamarque J-F, Lawrence PJ, Leung LR, Lipscomb W, Muszala S, Ricciuto DM, Sacks W, Sun Y, Tang J, Yang Z-L. 2013. Technical description of version 4.5 of the Community Land Model (CLM). NCAR Technical Note NCAR/TN-503+STR. <https://doi.org/10.5065/D6RR1W7M>.
- Osborn TJ, Hulme M. 1997. Development of a relationship between station and grid-box rainday frequencies for climate model evaluation. *J. Clim.* **10**(8): 1885–1908. [https://doi.org/10.1175/1520-0442\(1997\)010<1885:DOARBS>2.0.CO;2](https://doi.org/10.1175/1520-0442(1997)010<1885:DOARBS>2.0.CO;2).
- Pal JS, Giorgi F, Bi X, Elguindi N, Solmon F, Rauscher SA, Gao X, Francisco R, Zakey A, Winter J, Ashfaq M, Syed FS, Sloan LC, Bell JL, Diffenbaugh NS, Karmacharya J, Konaré A, Martinez D, da Rocha RP, Steiner AL. 2007. Regional climate modeling for the developing world: the ICTP RegCM3 and RegCM3. *Bull. Am. Meteorol. Soc.* **88**(9): 1395–1409. <https://doi.org/10.1175/BAMS-88-9-1395>.
- Reboita M, Fernandez J, Pereira Llopart M, Porfirio da Rocha R, Albertani Pampuch L, Cruz F. 2014. Assessment of RegCM4.3 over the CORDEX South America domain: sensitivity analysis for physical parameterization schemes. *Clim. Res.* **60**(3): 215–234. <https://doi.org/10.3354/cr01239>.
- Salimun E, Tangang F, Juneng L. 2010. Simulation of heavy precipitation episode over eastern Peninsular Malaysia using MM5: sensitivity to cumulus parameterization schemes. *Meteorol. Atmos. Phys.* **107**(1–2): 33–49. <https://doi.org/10.1007/s00703-010-0067-y>.
- Salimun E, Tangang F, Juneng L, Behera SK, Yu W. 2014. Differential impacts of conventional El Niño versus El Niño Modoki on Malaysian rainfall anomaly during winter monsoon. *Int. J. Climatol.* **34**(8): 2763–2774. <https://doi.org/10.1002/joc.3873>.
- Schär C, Lüthi D, Beyerle U, Heise E. 1999. The soil–precipitation feedback: a process study with a regional climate model. *J. Clim.* **12**(3): 722–741. [https://doi.org/10.1175/1520-0442\(1999\)012<0722:TSPFAP>2.0.CO;2](https://doi.org/10.1175/1520-0442(1999)012<0722:TSPFAP>2.0.CO;2).
- Schneider U, Becker A, Finger P, Meyer-Christoffer A, Ziese M, Rudolf B. 2014. GPCC's new land surface precipitation climatology based on quality-controlled in situ data and its role in quantifying the global water cycle. *Theor. Appl. Climatol.* **115**(1–2): 15–40. <https://doi.org/10.1007/s00704-013-0860-x>.
- Schumacher C, Houze RA. 2003. Stratiform rain in the tropics as seen by the TRMM precipitation radar. *J. Clim.* **16**(11): 1739–1756. [https://doi.org/10.1175/1520-0442\(2003\)016<1739:SRITTA>2.0.CO;2](https://doi.org/10.1175/1520-0442(2003)016<1739:SRITTA>2.0.CO;2).
- Siew JH, Tangang FT, Juneng L. 2014. Evaluation of CMIP5 coupled atmosphere-ocean general circulation models and projection of the Southeast Asian winter monsoon in the 21st century. *Int. J. Climatol.* **34**(9): 2872–2884. <https://doi.org/10.1002/joc.3880>.
- Steiner AL, Pal JS, Giorgi F, Dickinson RE, Chameides WL. 2005. The coupling of the common land model (CLM0) to a regional climate model (RegCM). *Theor. Appl. Climatol.* **82**(3–4): 225–243. <https://doi.org/10.1007/s00704-005-0132-5>.
- Steiner AL, Pal JS, Rauscher SA, Bell JL, Diffenbaugh NS, Boone A, Sloan LC, Giorgi F. 2009. Land surface coupling in regional climate simulations of the West African monsoon. *Clim. Dyn.* **33**(6): 869–892. <https://doi.org/10.1007/s00382-009-0543-6>.
- Sundqvist H, Berge E, Kristjánsson JE. 1989. Condensation and cloud parameterization studies with a mesoscale numerical weather prediction model. *Mon. Weather Rev.* **117**(8): 1641–1657. [https://doi.org/10.1175/1520-0493\(1989\)117<1641:CACPSW>2.0.CO;2](https://doi.org/10.1175/1520-0493(1989)117<1641:CACPSW>2.0.CO;2).
- Tangang FT, Juneng L. 2004. Mechanisms of Malaysian rainfall anomalies. *J. Clim.* **17**(18): 3616–3622. [https://doi.org/10.1175/1520-0442\(2004\)017<3616:MOMRA>2.0.CO;2](https://doi.org/10.1175/1520-0442(2004)017<3616:MOMRA>2.0.CO;2).
- Tiwari PR, Chandra Kar S, Mohanty UC, Dey S, Sinha P, Raju PVS, Shekhar MS. 2015. The role of land surface schemes in the regional climate model (RegCM) for seasonal scale simulations over Western Himalaya. *Atmosfera* **28**(2): 129–142. [https://doi.org/10.1016/S0187-6236\(15\)30005-9](https://doi.org/10.1016/S0187-6236(15)30005-9).

- Wang X, Yang M, Pang G. 2015. Influences of two land-surface schemes on RegCM4 precipitation simulations over the Tibetan plateau. *Adv. Meteorol.* **2015**: 1–12. <https://doi.org/10.1155/2015/106891>.
- Wang Y, Zhou L, Hamilton K. 2007. Effect of convective entrainment/detrainment on the simulation of the tropical precipitation diurnal cycle. *Mon. Weather Rev.* **135**(2): 567–585. <https://doi.org/10.1175/MWR3308.1>.
- Wei J, Malanotte-Rizzoli P, Eltahir EAB, Xue P, Xu D. 2014. Coupling of a regional atmospheric model (RegCM3) and a regional oceanic model (FVCOM) over the maritime continent. *Clim. Dyn.* **43**(5–6): 1575–1594. <https://doi.org/10.1007/s00382-013-1986-3>.
- Yan H, Anthes RA. 1988. The effect of variations in surface moisture on mesoscale circulation. *Mon. Weather Rev.* **116**(1): 192–208. [https://doi.org/10.1175/1520-0493\(1988\)116<0192:TEOVIS>2.0.CO;2](https://doi.org/10.1175/1520-0493(1988)116<0192:TEOVIS>2.0.CO;2).
- Yan Y, Xie Z-H. 2013. A simulation study on climatic effects of land cover change in China. *Adv. Clim. Change Res.* **4**(2): 117–126. <https://doi.org/10.3724/SP.J.1248.2013.117>.
- Yatagai A, Arakawa O, Kamiguchi K, Kawamoto H, Nodzu MI, Hamada A. 2009. A 44-year daily gridded precipitation dataset for Asia based on a dense network of rain gauges. *SOLA* **5**: 137–140. <https://doi.org/10.2151/sola.2009-035>.
- Zeng X, Zhao M, Dickinson RE. 1998. Intercomparison of bulk aerodynamic algorithms for the computation of sea surface fluxes using TOGA COARE and TAO data. *J. Clim.* **11**(10): 2628–2644. [https://doi.org/10.1175/1520-0442\(1998\)011<2628:IOBAAF>2.0.CO;2](https://doi.org/10.1175/1520-0442(1998)011<2628:IOBAAF>2.0.CO;2).
- Zou L, Qian Y, Zhou T, Yang B. 2014. Parameter tuning and calibration of RegCM3 with MIT–Emanuel cumulus parameterization scheme over CORDEX East Asia domain. *J. Clim.* **27**(20): 7687–7701. <https://doi.org/10.1175/JCLI-D-14-00229.1>.
- Zou L, Zhou T. 2013. Improve the simulation of western North Pacific summer monsoon in RegCM3 by suppressing convection. *Meteorol. Atmos. Phys.* **121**(1–2): 29–38. <https://doi.org/10.1007/s00703-013-0255-7>.